Crystallization and Melting of Model Ethylene−Butene Copolymers

B. Crist* and P. R. Howard†

Department of Materials Science and Engineering, Northwestern University, Evanston, Illinois 60208-3108

Received October 20, 1998; Revised Manuscript Received February 14, 1999

ABSTRACT: Crystallinity and melting behavior are directly affected by the presence of a noncrystallizable comonomer. Hydrogenated polybutadiene, HPB, emulates a random ethylene−butene copolymer and provides the basis for comparison to the equilibrium theory of Flory. Melting behavior, density (crystallinity), and SAXS long period were measured for HPB's having 12 to 88 ethyl branches per 1000 backbone C atoms. DSC curves calculated from equilibrium theory are compared to experimental traces. It is shown that the equilibrium melting temperature T_m^c of infinitely thick crystals, while thermodynamically correct, is inaccessible to experiment. Thickest crystals with observable populations melt at the practical final melting temperature T_m^f, which is below T_m^c. The peak melting temperature T_m^p has no relation to the most populous crystal thickness. Crystallization of molten copolymer chains leads to fewer thick and thin crystals than predicted by theory; the difference is attributed to kinetic factors of secondary nucleation barriers and mass transport. Crystallization at feasible rates is achieved when the melt is at a temperature low enough to undercool a sizable fraction of crystallizable segments. Crystallization prevents the motion of segments required to achieve equilibrium, so solidification proceeds as if the system were quenched, accounting for insensitivity of copolymer morphology to cooling rate. Only the size of the largest crystals which melt at experimental T_m^f can be established by thermodynamics. There is some evidence that small equilibrium crystallinities are approached in highly branched copolymers.

Introduction

Copolymerization of ethylene and α-olefins has long been used to synthesize polymers with controlled amounts of crystallinity and attendant physical properties (modulus, yield strength, fracture toughness, optical haze, etc.). There is consensus that most short-chain branches, which accompany enchainment of α-olefin comonomers, are rejected from the polyethylene-like crystals, thereby reducing both crystallinity and melting temperature. Conventional low-pressure catalysts give heterogeneous products, i.e., mixtures in which the concentration of α-olefin comonomer varies appreciably from chain to chain.[1] This complexity of chemical microstructure has impeded efforts to correlate morphology and properties with short-chain branching. For example, a conventional (heterogeneous) ethylene−butene copolymer with an average of 19 ethyl branches per 1000 carbon atoms has a melting temperature T_m = 126 °C,[2] about 20 °C higher than T_m for a homogeneous copolymer (all chains having the same branching) of the same comonomer composition.[3] The difference in this case is readily ascribed to the presence of thick crystals formed by essentially unbranched chains present in the heterogeneous system.

Although some attempts have been made to relate branch heterogeneity to the nature of partially crystalline copolymers,[2,4] the underlying understanding of simpler systems, with homogeneous branching, is still qualitative at best. Alamo and Mandelkern[5] have reviewed thoroughly copolymers of ethylene and α-olefins having uniform chemical microstructure. It is well established that melting temperature, crystallinity, and crystal thickness are reduced by the presence of short-chain branched repeat units. Morphology effects are independent of branch size (if larger than methyl, $-CH_3$), leading to the logical conclusion that such comonomer units are excluded from the crystalline regions. A number of questions remain unanswered: Can one predict from theory the melting temperature or crystallinity of a partially crystalline copolymer? Are experimental results consistent with theory? How robust is the popular two-phase model for copolymers? These and related issues are the focus of the present work, which is stimulated in part by the development of metallocene catalysts that give ethylene copolymers reported to have more homogeneous incorporation of α-olefin comonomers.[6]

Analyses of Copolymer Melting and Crystallinity

The most rigorous treatment is the equilibrium theory presented by Flory[7] over 40 years ago. The copolymer is composed of crystallizable A units (ethylene monomers) and noncrystallable B units (α-olefin monomers), and the probability of two A units being adjacent along the chain (the sequence perpetuation probability) is p. For random copolymers considered here, p is equated to the mole fraction of crystallizable A units. We will also use X_A, the *weight* fraction of A units (or the volume fraction of A in the molten copolymer). By considering thermodynamic equilibrium between crystals (composed of A units only) and the melt (composed of both A and B units), it is determined that crystals composed of sequences having the number of consecutive A units $n \geq n^*$ are stable at temperature T:

$$n^* = \frac{-1}{\theta + \ln p}\left[\ln\left(\frac{DX_A}{p}\right) + 2\ln\left(\frac{1-p}{1-e^{-\theta}}\right)\right] \qquad (1)$$

Here

$$\theta = \frac{\Delta H_u}{R}\left(\frac{1}{T} - \frac{1}{T_m^0}\right) \quad \text{and} \quad D = e^{-2\sigma_e a_o/RT}$$

† Present address: Schlumberger Cambridge Research, Cambridge CB3 0EL, U.K.

10.1021/ma9816362 CCC: $18.00
Published on Web 04/15/1999

express the undercooling and energetic consequences of basal surface energy, respectively. T_m^0 is the melting point for the perfect crystal (418.7 K for polyethylene[8]), ΔH_u is the heat of fusion for a repeat unit (8.284 kJ/mol for C_2H_4 units in polyethylene[9]), σ_e is the basal surface energy (90 mJ/m^2 for polyethylene[9]) and a_o is the cross-sectional area of a chain (1.10×10^5 m^2/mol for polyethylene[10]), all referred to crystals of homopolymer A. The basic idea is that noncrystallizable B units effectively partition the copolymer chains into A-runs of different n, which may associate to form crystals. Each crystal is composed of sequences with $n \geq n^*$, and is subject to a basal surface energy proportional to $1/n$. As this is a strictly equilibrium theory, crystallization and melting are both reversible.

The Flory model predicts correctly that copolymer melting occurs over lower and broader temperature ranges as p is decreased (comonomer content is increased). The thermodynamically defined melting temperature of the copolymer T_m^c corresponds to equilibrium between the thickest possible crystals ($n^* \rightarrow \infty$) and a melt having the global copolymer composition p:

$$\frac{1}{T_m^c} = \frac{1}{T_m^0} - \frac{R}{\Delta H_u} \ln p \qquad (2)$$

For any temperature $T < T_m^c$, the equilibrium crystallinity is calculated from the composition of the melt coexisting with crystals of sequence number $n \geq n^*(T)$. As the temperature is lowered, the critical sequence number $n^*(T)$ becomes smaller, the crystalline fraction increases by accretion of thinner crystals, and the melt becomes enriched in noncrystallizable B units. With the assumption that each A sequence of number n that has been removed from the melt is in a crystal of length nc ($c = 0.254$ nm for polyethylene), the weight fraction crystallinity f_c is

$$f_c = \frac{\sum_{n=n^*}^{\infty} (w_n^o - w_n^e)}{1 - \sum_{n=n^*}^{\infty} w_n^e} \qquad (3)$$

Here w_n is the probability that a unit selected randomly from the melt is an A unit that is part of a sequence of n consecutive A units, i.e., the weight fraction of n-sequences in the melt. Superscripts "o" and "e" refer to the completely molten copolymer and the melt in equilibrium with crystals, respectively. Additional relations, together with some comments on melting temperature, are presented in Appendices A and B. Equation 3 represents an upper bound for the cystallinity of a copolymer having A weight fraction X_A and sequence probability p. No allowance is made for chain connectivity, chain folding or other kinetic aspects. In the homopolymer limit, X_A and p approach 1, T_m^c approaches T_m^0, and crystallinity f_c approaches 1.

Examples of the temperature dependence of equilibrium crystallinity are shown in Figure 1a for ethylene−butene random copolymers (parameters as above, and $X_A = p/(2 - p)$ for this case when the volume of butene is twice that of ethylene). Equilibrium melting occurs over a large temperature range, raising the issue of what is meant by the "melting temperature". Be reminded that the thermodynamically defined T_m^c in eq 2 is for melting the thickest possible crystals ($n^* \rightarrow \infty$). The amount of such crystals is so small that this first-order transition temperature is impossible to measure, even in the unlikely event that thick equilibrium crystals are present. The temperature derivative of the crystallinity (Figure 1b) provides a link to experiment; in fact, $-df_c/dT$ is closely related to a differential scanning calorimetry (DSC) trace. Crystals melt as the critical sequence number $n^*(T)$ increases with temperature. Prominent in Figure 1b are the peak melting temperature T_m^p and the "final" melting temperature T_m^f, both of which are located below the thermodynamic T_m^c from eq 2. For the ethylene−butene copolymers considered here, T_m^p occurs at a crystallinity $f_c = 0.14$, and T_m^f at $f_c \approx 10^{-4}$. These characteristic crystallinities are not universal, being determined by the relation between surface energy σ_e and heat of fusion ΔH_u.

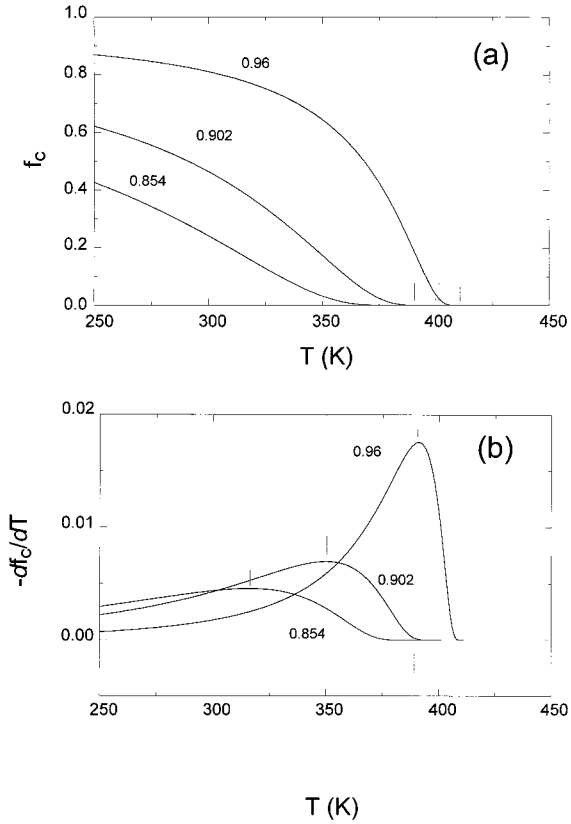

Figure 1. (a) Equilibrium crystallinity f_c as a function of temperature (eq 3) for random ethylene−butene copolymers having indicated values of p (mole fraction of ethylene monomer). Vertical lines near 400 K locate equilibrium T_m^c for the three copolymers. (b) Temperature derivative of curves in (a); upper vertical lines indicate peak melting temperatures (T_m^p) and lower lines give final melting temperatures (T_m^f) accessible to experiment.

Primarily because of the breadth of the melting range, curves such as those in Figure 1b do not reflect the distribution of crystal thickness. The same can be said of closely related DSC traces.[11,12] Figure 2 shows the desired distribution for a copolymer with $p = 0.96$ (20 ethyl branches/1000 backbone C atoms). Here $-df_c/dn^*$ is the probability density function for the weight fraction of crystals with thickness n^*. Temperature markers give a sense of how n^* increases more and more rapidly with temperature. This compression of melting the distribution at higher temperatures completely suppresses the maximum in $-df_c/dn^*$; the peak melting temperature at 391 K ($n^* \approx 70$) has no relation whatever to the most

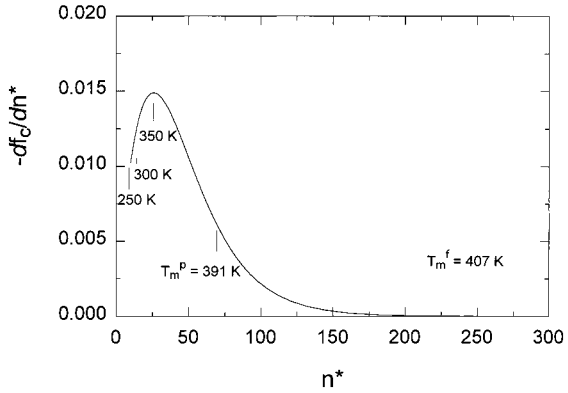

Figure 2. Equilibrium distribution of crystalline *n*-sequences in a random EB copolymer with $p = 0.96$, with certain temperatures indicated. Note that peak melting temperature T_m^p does not correspond to melting the most populous crystals.

populous crystals centered at $n^* = 25$, which melt around 350 K. T_m^p is the temperature where $f_c(T)$ has an inflection point—see parts a and b of Figure 1.

Other approaches to copolymer crystallization and melting have been proposed. Kilian[13] postulates that ordered domains are comprised of *n*-sequences of different lengths in "extended *c*-sequence mixed crystals", the disordered surfaces of which comprise the noncrystalline fraction ($1 - f_c$). With the aid of a number of phenomenological parameters, this "equilibrium" model can be fit to experimental melting curves for ethylene copolymers melting up to T ≈ 390 K. Kilian's contention that equilibrium is approximated during crystallization and melting of copolymers is not generally accepted. Simpler treatments of copolymers have been taken by Pakula[14] and Wang and Woodward,[15] who are concerned with the relation between average composition (p), crystallinity (f_c), and crystal thickness. Their method ignores thermodynamic equilibrium (melting is not addressed) and assumes that all sequences longer than some empirical value will crystallize, subject to other assertions about chain folding.

What amounts to a hybrid approach was taken by Sanchez and Eby.[16] For the case when comonomer B units are excluded from the crystals, the molar free energy of an A (ethylene) unit in a lamellar crystal having n_c units in the thickness direction is written as

$$\Delta G_c = \Delta H_u\left(\frac{T}{T_m^0} - 1\right) + \frac{2\sigma_e a_o}{n_c} - RT \ln p \qquad (4)$$

Here the copolymer nature of the chains is included in the last term involving ln p, which is accurate for vanishingly small crystallinity when the melt has the global copolymer composition p. The (final) melting temperature is that at which $\Delta G_c = 0$:

$$T_m^f = T_m^c\left(1 - \frac{2\sigma_e a_o}{\Delta H_u n_c}\right) \qquad (5)$$

T_m^c is given by eq 2. As there is no a priori relation between copolymer composition (p), crystal size (n_c) or temperature T, nonequilibrium lamellar crystals, with or without folds, may be treated with eq 5, which is Flory's equilibrium melting point for infinitely thick crystals (eq 2) modified in a standard manner for basal surface energy σ_e. Equation 5 furthermore provides an expression for analyzing the final melting temperatures T_m^f from Flory's equilibrium theory identified in Figure 1b. This relationship, which is illustrated in Appendix B, is employed here in analyses of experimental results.

Table 1. Chemical Characteristics of Model Polymers

polymer	p	$10^{-3}M_w$	M_w/M_n
PE	1.0	120	1.2
HPB-12	0.976	47	1.5
HPB-18	0.964	199	≤1.1
HBP-20	0.960	93	≤1.1
HPB-39	0.922	171	≤1.1
HPB-54	0.892	181	≤1.1
HPB-73	0.854	186	≤1.1
HPB-88	0.824	81	≤1.1

Experimental Section

Polymers. Model ethylene−butene (EB) copolymers are hydrogenated polybutadienes (HPB) with various amounts of 1,2-butadiene enchainments that lead to ethyl branches. Synthesis and characterization were as described by Rachapudy et al.[17] and by Howard and Crist.[18] The resulting polymers are nearly monodisperse ($M_w/M_n \leq 1.1$), are logically assumed to have the same average branching from chain to chain, and, most importantly, have intrachain branch placements that approximate ideal random EB copolymers.[3] It has been shown that ∼95% of the ethyl branches are excluded from the crystals.[19] Hence HPB's provide excellent systems for comparison to equilibrium copolymer theory.

Model copolymers are referred to as HPB-*xx*, where the suffix is the number of ethyl branches per 1000 backbone carbon atoms. This quantity is readily converted to the mole fraction of crystallizable C_2H_4 units, which is equal to p:

$$p = 1 - \frac{xx}{500}$$

For example, HPB-20 has 20 ethyl branches per 1000 backbone carbon atoms, and $p = 0.960$. A polyethylene fraction (NIST SRM 1484), designated PE, is used as an unbranched reference homopolymer. Molecular characterization is presented in Table 1. Molecular weights are reasonably similar, with the exception of HPB-12.

Samples were compression molded and either quenched in ice water (q) or slowly cooled (sc) to room temperature at about 1 °C/min. The more branched HPB's were drawn at room temperature and annealed with fixed ends at ca. 20 °C below their experimental T_m^f; this orientation treatment was required to obtain reasonable X-ray diffraction intensity.[18]

Physical Characterization. Densities were measured at 23 °C with a gradient column (2-propanol/water). Mass fraction crystallinity was calculated according to the standard two-phase model:

$$f_c = \frac{\rho_c}{\rho}\frac{\rho - \rho_a}{\rho_c - \rho_a}$$

Here ρ is the sample density and crystalline densities ρ_c and amorphous densities ρ_a were taken from earlier studies by Howard and Crist[18] and Krigas et al.[3] respectively.

DSC was done with Perkin-Elmer DSC2 or DSC7 instruments at a heating rate of 5 °C/min after cooling from the melt at 10 °C/min. Peak and final melting temperatures were recorded when feasible.

Small-angle X-ray scattering (SAXS) was performed on the 10 m instrument at Oak Ridge National Laboratories. Long period L was determined from Lorentz corrected (isotropic samples) or meridional (drawn samples) intensity profiles. The crystal thickness l_c was estimated from $l_c = L\varphi_c$, where $\varphi_c = f_c\rho/\rho_c$ is the volume fraction crystallinity from density.

Results

As has been shown many times before,[5] density decreases systematically with increased branching. The

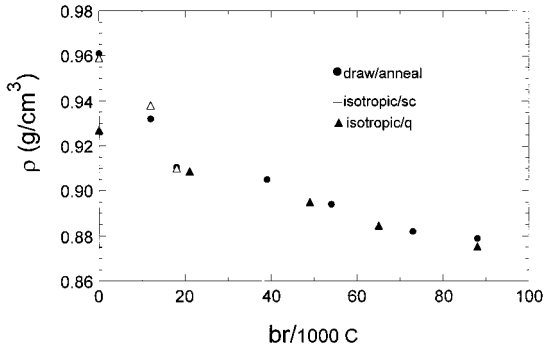

Figure 3. Density as a function of branching in HPB. Data for polymers with 20, 49 and 65 br/1000 C are from Krigas et al.[3]

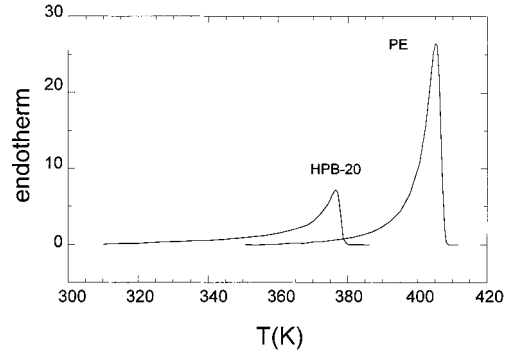

Figure 4. DSC traces for unbranched PE and HPB-20

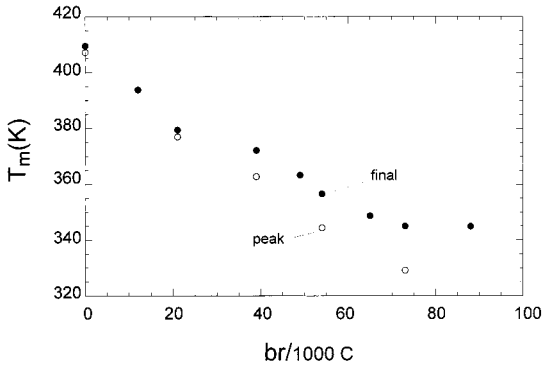

Figure 5. Melting temperatures as a function of branching for HPB's.

Table 2. Experimental Results for Model EB Copolymers

		crystallization				melting	
copolymer	p	T_x (K)[a]	l_x (nm)[b]	f_m at T_x	f_c at T_x	T_m^f (K)	l_f (nm)[b]
HPB-12	0.974	379	7.1	0.82	0.64	394	12.3
HPB-18	0.964	372	6.2	0.73	0.52	384	8.8
HPB-20	0.960	369	5.9	0.71	0.49	380	7.9
HPB-39	0.922	351	4.6	0.50	0.29	372	7.5
HPB-54	0.892	336	3.8	0.41	0.22	357	5.7
HPB-73	0.854	323	3.3	0.29	0.14	345	5.0
HPB-88	0.824	320	3.5	0.19	0.07	345	5.6

[a] Temperature at which crystallization first occurs in DSC experiment.[3] [b] $l = n_c c$, with n_c from eq 5 at T_x or T_m^f.

Table 3. Physical Characteristics of Model Copolymers

	experiment					equilib theory		
copolymer[a]	ρ (g/cm3)	f_c	l_c (nm)[b]	T_m^f (K)[c]	l_f (nm)[d]	f_c	l^* (nm)[e]	T_m^f (K)
HPB-12sc	0.938	0.65	10.4	394	12.3	0.90	11.3	411
HPB-12	0.930	0.61	9					
HPB-18sc	0.910	0.45	6.2	384	8.8	0.83	7.3	408.5
HPB-39	0.905	0.43	6.2	372	7.5	0.58	3.6	396
HPB-54	0.894	0.34	4.6	357	5.7	0.41	3.5	387.5
HPB-73	0.882	0.23	3.2	345	5.0	0.24	3.5	376
HPB-88	0.879	0.18	2	345	5.5	0.14	3.6	367

[a] All samples drawn and annealed unless designated sc for isotropic, slow cooled. [b] $l_c = L\varphi_c$ from long period and volume fraction crystallinity from density. [c] DSC samples crystallized during −10 °C/min cooling. [d] From experimental T_m^f and eq 5 (Table 2). [e] Most probable crystal size at 300 K.

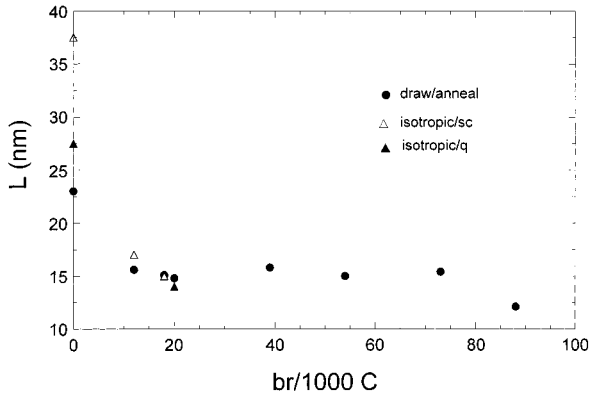

Figure 6. SAXS long period as a function of branching for HPB's.

data in Figure 3 further underscore that the density of a semicrystalline copolymer is rather insensitive to thermal or mechanical history, with changes on the order of 0.004 g/cm3. Unbranched PE, on the other hand, displays density changes nearly 10 times larger when subjected to the same histories. Homopolymer morphology (crystallinity) is subject to a level of kinetic control not seen in copolymers.

The basis for thermal analysis is shown by DSC traces for PE and HPB-20 in Figure 4. Branching shifts the melting range to lower temperatures and conspicuously lowers the magnitude of the endotherm. Not so obvious is the low temperature tail on the DSC trace of HPB-20. This feature, which is qualitatively consistent with the curves in Figure 1b, complicates establishment of a baseline for estimating the heat of fusion of the copolymer. Final and peak melting temperatures are nevertheless relatively well defined. As shown in Figure 5, these decrease with increased branching. A related observation is that the difference between peak and final melting temperatures increases with branching, again in qualitative accord with equilibrium theory (see Figure 1b), which predicts a broader melting range with decreasing p. The melting temperature for the most branched HPB-88 ($p = 0.824$) is larger than expected, being the same as $T_m^f = 345$ K for HPB-73. One should not conclude that the melting temperature becomes independent of branch concentration, because recent studies give $T_m^f = 334$ K for HPB-106.[20] Krigas et al.[3] also found that the final melting temperature of the same HPB-88 polymer was anomalously high. We have no explanation for this minor disruption of the pattern. Other characteristics such as density (Figure 3) and crystal thickness from SAXS (Table 3 below) indicate that HPB-88 indeed has more branching than HPB-73. Only the melting behavior seems irregular.

Alternating crystalline−amorphous domains have a periodicity given by the SAXS long period L, shown in Figure 6. This measure of the morphology decreases substantially on incorporation of the smallest amount of branching (HPB-12) and remains nearly constant around 15 nm as branching is increased. As with

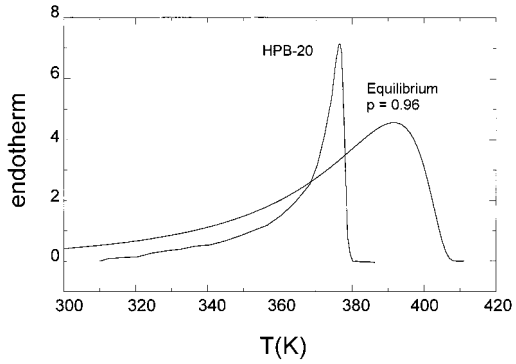

Figure 7. Experimental and calculated (equilibrium) DSC traces for HPB-20.

density, thermal and mechanical history have virtually no effect on L for the copolymers, whereas the long period is very history dependent for unbranched PE.

Discussion

A revealing comparison of an actual copolymer to equilibrium predictions is provided in Figure 7, which displays the DSC trace for HPB-20 and that calculated from eq 3. Here $-\mathrm{d}f_c/\mathrm{d}T$ has been scaled by a heat of fusion proportional to T/T_m^c, an approximate correction for thin lamellar crystals in copolymers. Aside from low area (crystallinity) for HPB-20, obvious differences are the absence of crystals melting above 380 K and a deficiency below ~350 K. One feature which has not, to our knowledge, been reported before is the DSC trace exceeding the calculated endotherm in the vicinity of the experimental T_m^p. The picture that emerges was described in part by Flory and co-workers:[7,21] The thickest (highest melting) equilibrium crystals do not form because of kinetic constraints associated with transport and nucleation of long n-sequences as discussed below. These longest sequences (or portions thereof) crystallize at a lower temperature, together with shorter segments that are also adequately undercooled. This nonequilibrium primary crystallization leads to narrower distribution of crystal sizes that exceeds the equilibrium population at the experimental T_m^p. At this point the remaining amorphous n-sequences are constrained by the primary crystals, hindering the formation of thinner crystals as temperature is decreased further. Hence the experimental DSC curve falls below equilibrium at lower temperatures.

A more quantitative picture of this departure from equilibrium can be developed as follows. From Figure 7 we establish $T_m^f = 407$ K as the practical temperature below which equilibrium crystals are present in a copolymer with $p = 0.96$. From Figure 2 we see that crystals corresponding to equilibrium melting at $T_m^f = 407$ K have $n^* = 250$, or crystal thickness $l^* = 63$ nm. There is abundant evidence that secondary nucleation barriers to the growth of such thick crystals are very large. Add to this the fact that these longest n-sequences are present at a concentration on the order of 0.01 wt %, which signifies serious transport issues. One can appreciate that kinetic impediments to the formation of these thickest observable equilibrium crystals from very dilute, long n-sequences are formidable indeed. This conclusion is supported by data in Figure 6 for unbranched PE, with no thermodynamic restrictions on sequence lengths, for which crystals thinner than 30 nm are formed.

With appropriate long time isothermal experiments it might be possible to form some copolymer crystals with $l_c \approx 63$ nm corresponding to the equilibrium T_m^f. However, the very first stage of crystallization involving the longest n-sequences pins each chain at least once in a crystal. Depending on details of molecular weight and sequence probability p, this piecewise crystallization of copolymer molecules would soon establish a network of entangled subchains composed of shorter n-sequences running between crystals, at which point the system is topologically frustrated from achieving larger equilibrium crystallinity at longer times or lower temperatures. Such an effect is shown clearly in the isothermal studies by Alamo and Mandelkern[22] on model copolymers similar to HPB-20. Crystallization at temperatures 368 K-383 K exhibits abrupt deceleration at $f_c \leq 0.1$, well short of equilibrium crystallinities of 0.3−0.4. Homopolymer PE of the same molecular weight readily crystallizes to $f_c \approx 0.8$, much closer to the equilibrium value of unity, under comparable isothermal conditions.[23]

Granted that crystallization of a random copolymer will fall well short of equilibrium predictions, what information can be established from composition p, n-sequence distribution, and thermodynamics? We use eq 5 at a particular temperature for equilibrium between *completely molten* copolymer having the global n-sequence distribution w_n^o (see eq A1 in Appendix A) and crystals of thickness $l = n_c c$. This approach is applicable to analysis (but not to prediction) of both initial crystallization temperatures T_x and final melting temperatures T_m^f, as the crystalline fraction is insignificant in both cases and the mole fraction of ethylene units in the melt is essentially equal to p. We now return to experiments on HPB-20, for which DSC indicates crystallization over a ca. 5 K range starting at 369 K.[3,20] Substituting $T_x = 369$ K for T_m^f in eq 5, one finds that crystals with $n_c = 23$ are in equilibrium with completely molten copolymer, or that n-sequences with $n > 23$ are undercooled at 369 K. When referred to the overall sequence distribution w_n^o for the random copolymer with $p = 0.96$, Figure 8a reveals that crystallization first occurs at a temperature low enough to stabilize crystals having the most probable sequence length. Furthermore, at this temperature the fraction of undercooled sequences in the melt is $f_m = 0.71$, so concentration is no longer a major issue. An unknown portion of these segments with $n > 23$ form crystals of length greater than $l_x = 23c = 5.9$ nm.

It is important to distinguish between two types of equilibrium between thin crystals and molten copolymer. The Flory model is for a *semicrystalline* polymer with equilibrium crystallinity f_c, which may be as large as X_A at very low temperatures. These stability relations are for crystals of thickness $l^* = n^*c$ in equilibrium with the coexisting melt, the composition of which is less than p due to removal of crystallizable A (ethylene) units. The Sanchez−Eby relation is for crystals of thickness $l = n_c c$ in equilibrium with a melt of *global* composition p, which applies only when $f_c \approx 0$. Primary crystallization increases f_c, which in turn changes the melt composition and the stability relations established in the preceding paragraph. For illustration only, assume the limiting case when equilibrium crystallinity $f_c = 0.52$ is achieved isothermally at 369 K. The coexisting melt is enriched by a factor of ~2 in noncrystallizable butene units, and the minimum stable crystal thickness in the semicrys-

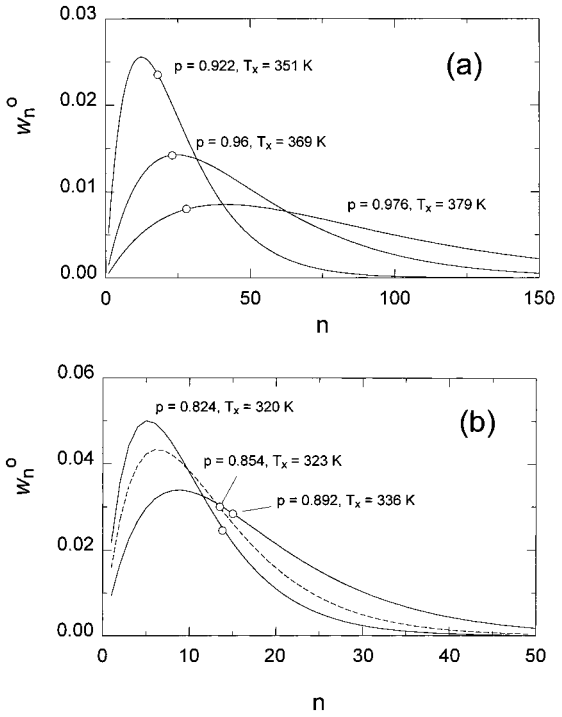

Figure 8. Overall (melt) distribution of *n*-sequences for random EB copolymers indicated values of composition *p*. Open circles indicate crystal thickness from eq 5 in equlibrium with undercooled melt at experimental crystallization temperature T_x for the corresponding HPB's. Segments corresponding to distribution maxima for more branched copolymers in part b are undercooled only below room temperature.

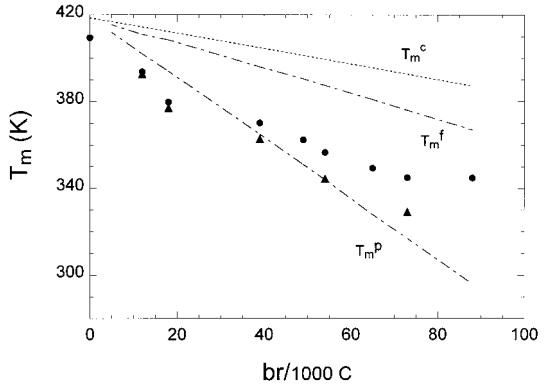

Figure 9. Comparison of experimental peak (▲) and final (●) melting temperatures to equilibrium values for EB copolymers having different amounts of branching.

talline polymer corresponds to $n^* = 38$, considerably larger than $n_c = 23$ for stability with the global melt. Any thin crystals initially formed with $23 \leq n < 38$ would melt as equilibrium is approached. For this reason the equilibrium crystallinity $f_c = 0.52$ is less than $f_m = 0.71$, the fraction of *n*-sequences that were undercooled with respect to the global melt at $T_x = 369$ K.

Following primary crystallization of HPB-20 in the range just below $T_x = 369$ K, some additional, and presumably thinner, crystals are formed on cooling to room temperature. We know only that the crystallinity at 300 K will be less than the equilibrium $f_c = 0.81$ (see Figure 1a). However, the experimental *final* melting temperature establishes unambiguously the size of the thickest crystals present in observable quantity. For HPB-20 we have from DSC that $T_m^f = 380$ K. With eq 5 this implies that the largest (nonequilibrium) crystals have $n_c = 31$ or thickness $l_f = 7.9$ nm. Hence crystallization of HPB-20 at $T_x \approx 390$ K forms crystals with 5.9 nm $< l \leq$ 7.9 nm. These estimates of crystal thickness from eq 5 neglect energy penalties associated with lateral surfaces. This approximation is often justified because the lateral surface energy σ is only a fraction of the basal surface energy σ_e,[9] and the lateral surface area is small in lamellar crystals. We assert that thin crystals in HPB are in fact lamellar (transverse width much greater than *l*) because of the existence of coherent stacks that give rise to discrete SAXS patterns.

Analyses of experimental crystallization and final melting of the other model copolymers give similar results presented in Table 2 and in Figure 8. In all cases crystallization at T_x is seen to involve an appreciable portion f_m of undercooled molten copolymer, and corresponding crystal thicknesses are in the kinetically feasible range from about 3 to 12 nm. It should be noted that experimental T_x does not generally correspond to stabilizing the most probable *n*-sequences. The least branched copolymer ($p = 0.976$) has a broad maximum in Figure 8a at $n = 41$ or $l = 10.4$ nm; experimental undercooling seems to select *n*-sequences about 30% shorter than this. Maxima in w_n^o are achieved on cooling to or below room temperature (represented by $n \approx 8$) for the copolymers with $p < 0.9$ in Figure 8b.

Regardless of details, the picture that emerges is a reasonable one. The molten copolymer crystallizes when the temperature T_x is low enough to establish thermodynamic undercooling for an appreciable fraction f_m of the molten *n*-sequences. For all EB copolymers considered here, the smallest undercooled *n*-sequences have lengths $l_x \leq 7.1$ nm, meaning that nucleation barriers to growth of thin stable crystals are moderate. Primary crystallization of the undercooled melt leads to somewhat thicker crystals from longer *n*-sequences, some of which may fold. One notes that the maximum crystal thickness l_f derived from T_m^f is about 1.6 l_x. Primary crystallization also pins uncrystallized segments and hinders further crystallization on subsequent cooling. Even a qualitative assessment of additional crystallization from the highly constrained system is speculative. The minimum crystal thickness stable at room temperature is about 3.5 nm in the equilibrium model for the amounts of branching considered here. Actual crystals may be thinner because lower experimental crystallinities imply the metastable melt has a composition closer to *p*, stabilizing smaller crystals.

We continue with a brief comparison of HPB characteristics to predictions of equilibrium theory. Experimental and calculated melting temperatures are shown in Figure 9. The upper dotted line is the thermodynamic melting temperature T_m^c from eq 2, which is inaccessible to experiment. T_m^f from equilibrium theory is well above the experimental points, an effect ascribed to kinetic factors as described above. Experimental peak melting temperature T_m^p, on the other hand, agrees fairly well with theory for copolymers with ~40 branches/1000 C or more. Note that all three definitions of melting temperature from the equilibrium model, T_m^c, T_m^p, and T_m^f, appear to be linear with respect to branch concentration. The relation between T_m^c and branching can be deduced from eq 2. Linearity of T_m^f and T_m^p vs branching reflects an implicit self-similarity in melting of random copolymers with different comonomer contents.

Room-temperature crystallinities (from density) are plotted along with equilibrium predictions in Figure 10.

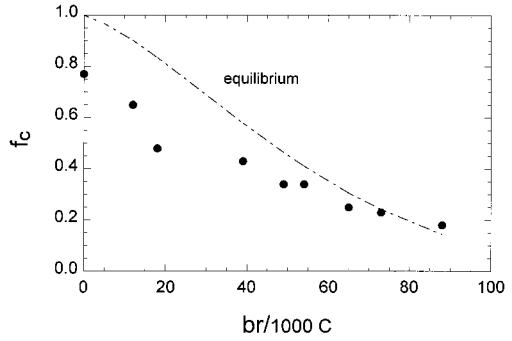

Figure 10. Comparison of experimental crystallinity (from density) to equilibrium values for EB copolymers having different amounts of branching..

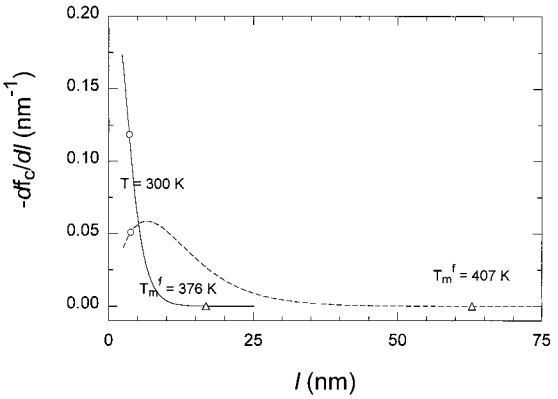

Figure 11. Equilibrium crystal length distribution for random EB copolymers with $p = 0.96$ (- -, HPB-20) and $p = 0.854$ (—, HPB-73). Points indicate crystal sizes melting 300 K (○) and at respective values of T_m^f (△).

Here again agreement is reasonable for higher levels of branching. Experimental crystallinity from calorimetry of HPB's also converges to f_c from the Flory model at branching in excess of 100 br/1000 C.[20] Is it logical that highly branched copolymers conform rather closely to f_c and T_m^p for the equilibrium model? We reiterate that high-temperature melting, either true equilibrium T_m^c or the experimentally accessible equilibrium T_m^f, is not approached in these experiments, nor is it approached after melt crystallization for days at small undercoolings.[24,25] However, more branched copolymers have less equilibrium crystallinity at room temperature and a *n*-sequence distribution that is more sharply peaked at small *n*. Both these factors contribute to fewer impediments to obtaining, or at least approaching, the equilibrium state at room temperature. Comparison of HPB-20 ($p = 0.96$) and HPB-73 ($p = 0.854$) in Figure 11 is instructive in this regard. Shown are the equilibrium crystal thickness distributions; room temperature crystallinity is recovered by integrating the curves from the point for $T = 300$ K. For the highly branched case ($p = 0.854$) one sees that virtually all crystallinity $f_c = 0.24$ is provided by crystals (or *n*-segments) of length $l \leq 10$ nm. Again we assert that secondary nucleation of such short *n*-segments is feasible in laboratory time scales. Something close to equilibrium could occur on cooling this highly branched copolymer because there are no "long" *n*-sequences that can slow or otherwise hinder crystallization. In contrast, over half of the equilibrium crystallinity $f_c = 0.81$ in the less branched copolymer ($p = 0.96$) derives from crystals with 10 nm $\leq l \leq 35$ nm. While these long sequences needn't form extended chain crystals, one anticipates that kinetic factors will limit their participation in primary crystallization.

Regardless of the qualitative arguments in the preceding paragraph, consideration of melting as well as crystallinity weakens the conclusion that equilibrium is approached in highly branched copolymers. Recall that experimental T_m^f is always well below the equilibrium prediction (see Figure 9), regardless of branching. For HPB-73 the experimental T_m^f shows that the thickest crystals have $l_f = 4.7$ nm or $n_c = 18.5$ (Table 2). For this to be compatible with equilibrium crystallinity $f_c = 0.24$, longer *n*-sequences must participate in crystals with $l \leq 4.7$ nm with full contribution to crystallinity, i.e., with "tight folding", which is thought to be unlikely. For HPB-88, $f_c = 0.18$ from density, which in fact exceeds the equilibrium crystallinity.

There are at least two explanations for such inconsistencies. The first is that experimental crystallinity from density or any other method is inexact for small values of f_c. While the density ρ itself is precise, the derived f_c is subject to uncertain phase densities, particularly ρ_a. Alamo and Mandelkern[5,25] conclude that f_c from density is erroneously larger than estimates from heat of fusion due to a crystal-amorphous interfacial zone having an effective density equal to ρ_c, but a liquidlike enthalpy. We see the same sort of differences[20] but suspect that accurate integration of broad endotherms (see Figure 4) is problematic. In short, unambiguous measurement of small f_c is difficult if not impossible. A second factor that confounds detailed comparison of experiment to theory is the value of "*p*" in the Flory theory. Krigas et al.[3] have pointed out that while the branch distribution in HPB's closely approximates expectations for random EB copolymers, this equivalence cannot be exact. This being the case, a value of *p* different from the effective butene concentration should be used and equilibrium f_c, T_m, etc. should be changed by unknown amounts.

Unlike crystallinity, the experimental peak melting temperature T_m^p is unambiguous. However, T_m^p only indicates the inflection point of crystallinity vs T and conveys no reliable information on crystal length, crystal size distribution, etc. Equilibrium for highly branched copolymers is characterized by a gradual decrease in f_c with T, leading to a broad endotherm (Figure 1). Nonequilibrium crystallization suppresses the high-temperature part of the crystal size distribution, and it is not surprising that experimental T_m^p (the inflection point) occurs at or even above the equilibrium T_m^p. Such behavior is seen in Figure 9 and has little significance.

The final measure of crystal thickness is that obtained from the SAXS long period and room-temperature volume fraction crystallinity φ_c in Table 3. Notice that l_c decreases, as expected, with increased branching. It is reasonable that the SAXS measure of crystal thickness is less than the maximum l_f from the final melting temperature. Comparison to theory is provided by the most probable equilibrium values l^* in Table 3. The significance of experimental l_c for highly branched copolymers is open to question. If measured (overall) crystallinity is too large, this will of course inflate the apparent crystal thickness. However, it is almost certain that the overall crystallinity is less than the local crystallinity within crystalline-amorphous stacks that give rise to the long period L because the stacks are not volume filling. Hence the calculated l_c from SAXS and crystallinity is likely too small for HPB-73 and HPB-

88. Other estimates of l_c could be obtained from more detailed consideration of the SAXS profile; these have not been performed in the present work.

Insight on the origin of the nonequilibrium state can be gained from the fact that room-temperature crystallinity (Figure 3) and long period (Figure 6) are insensitive to crystallization conditions. Recall that morphology is largely established during primary crystallization at or slightly below T_x when cooling to room temperature. We again consider HPB-20, for the estimated time for primary crystallization varies between about 300 s (slow cooling) to less than 1 s (quenching). At $T_x = 369$ K some 71% of the *n*-sequences are undercooled (Figure 8a). One conceivable product of primary crystallization around this temperature is the equilibrium state with $f_c = 0.51$, crystals extending to $l = 63$ nm and melting at $T_m^f = 407$ K, as described above. Even if secondary nucleation barriers are neglected, achievement of equilibrium requires impossible diffusion of the crystallizing segments. At the other extreme is a nonequilibrium state established by primary crystallization of neighboring *n*-segments, regardless of length, provided they are longer than $l_x = 5.9$ nm, with essentially no transport of chains or sections thereof. Any representative crystallite would include both short and long *n*-sequences, the latter folding or attaching in nearby crystals as in melt crystallization of homopolymer. The resulting nonequilibrium crystallinity will be below the equilibrium f_c by an unknown amount. One can predict, however, that kinetically controlled crystallization will favor crystal thicknesses somewhat above the limiting $l_x = 5.9$ nm.

One might expect a transition from the "quench crystallized" state toward equilibrium, with larger f_c and T_m^f, when more time is allowed for crystallization during slow cooling. This is true, however, only if the sort of chain mobility that permits approach to equilibrium in fact occurs. The present results indicate that the ca. 300 s provided by slow cooling is inadequate to allow a significant amount of transport that would lead to more crystallinity and thicker crystals, which is why crystallinity and long period are essentially unchanged by cooling rate. We posit, but cannot prove, that the segmental transport in question is suppressed by the first stages of crystallization. Should this be so, all copolymer melt crystallizations are effectively of the "quenched" sort, well short of equilibrium predictions. One should not infer that no morphological differences accompany changes in crystallization rate but that effects in copolymers are very small when compared to homopolymers. Slow cooling copolymers does increase the width of lamellar crystals.[26]

Independent evidence for lack of chain mobility in laboratory time scales is provided by small-angle neutron scattering (SANS). Quenching or slow cooling HPB-20 blended with its deuterated analogue leads to no changes in the SANS pattern.[27] Specifically, the radii of gyration of copolymer chains are the same in the melt, after quench crystallization, and after slow cooling. Furthermore, slowly cooled blends show no evidence of segregation of normal and deuterated chains, which remain statistically mixed in the semicrystalline state. These observations are consistent with the idea that piecewise crystallization of copolymer molecules effectively curtails transport, which leads naturally to insensitivity to crystallization conditions. In a homopolymer, there is no chemically determined distribution of segment lengths; all sections of all chains may crystallize, subject only to the usual stability conditions for lamellar crystals. Here a larger cooling rate increases the experimentally imposed crystallization rate, and the latter is achieved by the growth of thinner crystals. This more rapid growth invariably reduces the crystallinity as well, for reasons that are qualitatively if not precisely understood.[9,22] While diffusive transport (as opposed to local rearrangement) is not required for melt crystallization of PE, SANS observation of segregation of normal and deuterated chains after slow crystallization[28] shows that "long range" mobility is present while the homopolymer is solidifying.

Because the chain mobility required to achieve the equilibrium semicrystalline state is suppressed by early stages of crystallization, entangled molten copolymer chains solidify to the extent possible by effective "quench crystallization", regardless of temperature−time schedule. This concept was first introduced by Wunderlich[29] to describe copolymer crystallization close to the glass transition temperature, but we believe that mobility is limited well above T_g. Alamo and Mandelkern[22] later proposed a similar idea which emphasizes the role of trapped entanglements, analogous to the situation in high molecular weight homopolymer.

Conclusions

Equilibrium consideration of the crystal to liquid melting transition has two functions; establishing conditions (e.g., temperature) for the existence of the most stable phase, and providing a framework for kinetic treatments of crystallization to various metastable states. Hoffman and Miller[9] have developed these ideas in considerable detail for unbranched polyethylene, while Keller and Goldbeck-Wood[30] have reviewed a broader selection of flexible chain homopolymers. A fair assessment of the current state is that the relation between growth rate and thickness of lamellar crystals formed from undercooled melts or solutions is well established in terms of secondary nucleation theory, although a number of details are still under discussion. Missing, however, is a quantitative understanding of why the (metastable) crystallinity in homopolymers is less than unity, an effect exacerbated by rapid crystallization at large undercoolings, and by long polymer chains.

The more complex case of random copolymers has received relatively little attention. Equilibrium is certainly more challenging to describe; in place of $f_c = 0$ (above T_m^0) or $f_c = 1$ (below T_m^0) for the homopolymer, one has temperature-dependent crystallinity and distributions of crystal thickness as in Figure 1a and Figure 2. It has been recognized since the earliest experiments on copolymer crystallization and melting that Flory's[7] equilibrium theory accounts in a qualitative manner for reduced crystallinity and lower and broader melting ranges when comonomer content is increased, but quantitative agreement is lacking with laboratory observations. From the present consideration of theory and limited experiments we can draw the following conclusions.

1. The Flory theory[7] is the best available for copolymer equilibrium crystallization and melting (see Appendix B). Equilibrium crystallization (and hence melting) is not achieved because of kinetic constraints deriving from limited transport of chain segments and secondary nucleation barriers. Equilibrium T_m^c (eq 2)

should be replaced by the lower temperature T_m^f for comparison to experimental melting or calculating driving forces for crystallization. This reduces, but does not eliminate, the discrepancy between calculated and observed melting points.

2. The Sanchez−Eby expression (eq 5) is applicable to *final* melting of nonequilibrium crystals. It also applies to the first stages of nonequilibrium crystallization in an undercooled copolymer melt. Quantitative treatment of nonequilibrium crystal melting is not possible at present. The shapes of DSC or other melting curves do not give reliable estimates of crystal thickness distributions because melting is governed by both crystal thickness and melt composition, the latter being unknown for nonequilibrium cases.

3. Primary nonequilibrium crystallization is seen to occur at temperatures that stabilize crystals with thickness $l_x \leq 7$ nm. Under these conditions secondary nucleation barriers are moderate and a sizable fraction of *n*-sequences are undercooled, both factors being important for kinetic reasons. Segmental mobility, which is required to achieve equilibrium crystallinity, is suppressed by the earliest stages of crystallization.

4. Because segmental transport is virtually absent, crystallization of random copolymers from the melt is effectively of the "quenched" sort, regardless of the time scale allowed for the phase transformation. Morphology of the copolymer therefore is insensitive to crystallization conditions.

5. Experimental room-temperature crystallinity appears to approach equilibrium f_c in highly branched copolymers that have low crystallinity and relatively few topological restrictions to achieving the equilibrium state. However, absolute crystallinities and the important model parameter "*p*" are not known with adequate precision to confirm the significance of this observation.

Acknowledgment. This research was supported in part by the National Science Foundation through the Northwestern University Materials Research Center, and by the Gas Research Institute, Basic Sciences Division.

Appendix A. Equilibrium Crystallinity of Copolymers

Equation 3 in the text for copolymer crystallinity is based on probabilities w_n that a monomer chosen at random from the melt is an A unit in a sequence of *n* consecutive A units. For the completely molten copolymer one has[7]

$$w_n^{\circ} = n\frac{X_A}{p}(1-p)^2p^n \tag{A1}$$

For an amorphous polymer in equilibrium with crystals of sequence numbers *n*, $n+1$, and $n+2$, Flory showed that the coexisting melt must conform to

$$w_n^{e} = \frac{n}{D}(1-e^{-\theta})^2e^{-n\theta} \tag{A2}$$

The critical sequence number n* (eq 1 in text) is obtained by equating w_n° and w_n^{e}.

Crystallinity is calculated by comparing the concentration of *n*-sequences of crystallizable A units in the coexisting melt with those in the completely amorphous homopolymer:

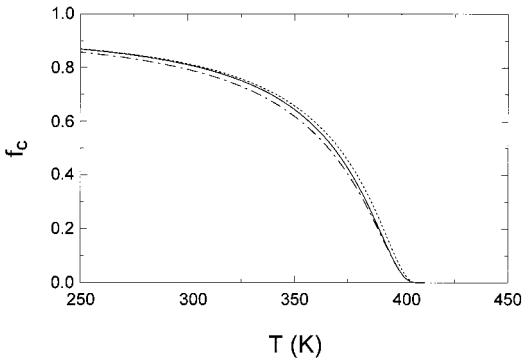

Figure 12. Crystallinity as a function of temperature for a model EB copolymer, $p = 0.96$: (—) f_c from eq A4, used in this work; (— - —) f_c from Flory;[7] (- -) f_c^{max} from eq A5.

$$f_c = \sum_{n=n^*}^{\infty}[w_n^{\circ} - (1-f_c)w_n^{e}] \tag{A3}$$

The sum is restricted to $n \geq n^*$ because only sequences of those lengths can participate in stable crystals. Flory omitted the factor $(1 - f_c)$, which is required because the amount of amorphous copolymer is reduced by the presence of crystals. This deficiency was pointed out by Kilian,[31] Baur,[32] and Wunderlich.[33] Equation A3 is rearranged to give eq 3 in the text. On substituting for w_n°, w_n^{e}, and *D*, the result is

$$f_c = \frac{\frac{X_A}{p}(1-p)^2p^{n^*}\left[\frac{p}{(1-p)^2} - \frac{e^{-\theta}}{(1-e^{-\theta})^2} + n^*\left(\frac{1}{(1-p)} - \frac{1}{(1-e^{-\theta})}\right)\right]}{1 - \frac{X_A}{p}p^{n^*}\left(\frac{1-p}{1-e^{-\theta}}\right)^2[n^*(1-e^{-\theta}) + e^{-\theta}]} \tag{A4}$$

This expression differs from eq 18 in ref 7 by the second term in the denominator, which is absent in Flory's treatment. An example of the effect on calculated crystallinity is shown in Figure 12. Also included in Figure 12 is the quantity

$$f_c^{max} = \sum_{n=n^*}^{\infty} w_n^{\circ} = X_A[n^*p^{n^*-1} - (n^*-1)p^{n^*}] \tag{A5}$$

which is the maximum possible crystallinity at temperature *T*, i.e., the weight fraction of *n*-sequences in the copolymer having $n \geq n^*$.

One sees in Figure 12 that the difference between the Flory and correct treatments are small, even when the crystallinity is appreciable. The two methods of course converge at high temperatures when $1 - f_c \approx 1$. When crystallinity is large (low temperatures) the Flory result is still reasonably accurate, because nearly all the supercritical sequences ($n \geq n^*$) have crystallized, and the w_n^{e} in eq A3 are small and unimportant. This is confirmed by the fact that $f_c \approx f_c^{max}$, the maximum crystallinity. Such efficient partitioning of supercritical *n*-sequences will not occur for copolymers in which the surface energy σ_e is small, and differences between Flory and eq A4 will be more significant.

Appendix B. Melting Temperature of Copolymers

Equation 5 in the text, from Sanchez and Eby,[16] provides a basis for experimental characterization of nonequilibrium copolymer crystals. The robustness of

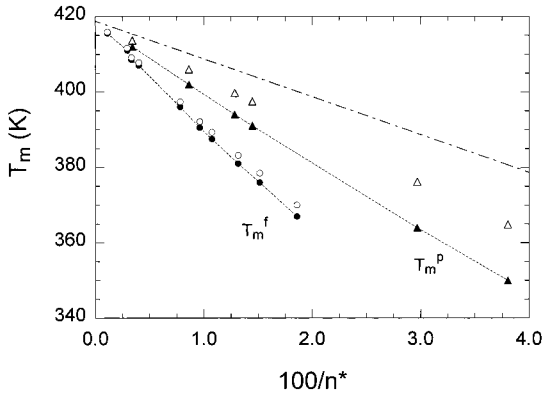

Figure 13. Melting temperature as a function of reciprocal crystal thickness, indicated by $1/n^*$, for EB copolymers with p ranging from 0.99 (highest T_m) to 0.824 (lowest T_m). Solid points are from the equilibrium model (e.g. Figure 1b): (▲) T_m^p; (●) T_m^f. Open points are calculated from eq 5 with $n_c = n^*$(peak) (△) or $n^* = n_c$(final) (○). The dashed line is for surface energy only (eq 5 in text with $p = 1$).

this approach is examined in terms of equilibrium theory for ethylene−butene copolymers with p between 0.99 and 0.824. Calculated curves of $-df_c/dT$ were used to establish T_m^p and T_m^f, together with the corresponding values of n^*, the sequence number of crystals melting at these temperatures. In Figure 13 it is seen that both choices of melting temperature have different, nearly linear dependencies on $1/n^*$. In neither case does this apparent "Gibbs−Thompson" behavior lead directly to the surface energy σ_e, which is given by the smaller slope of the dashed line. Equilibrium copolymer crystals have a steeper slope in this format because smaller p (more branching) simultaneously shifts the crystal size distribution to smaller values of $l^* = n^*c$ (more surface energy penalty) and lowers the "infinite crystal" limit T_m^c in eq 2.

As the thermodynamics underlying eq 5 in the text implicitly assumes $f_c \approx 0$, this expression was used with n^*(final) substituted for n_c. Points so calculated agree quite well with T_m^f from equilibrium theory in Figure 13; slight discrepancies at larger branching are due to residual crystallinity ($f_c \approx 10^{-4}$) at T_m^f, which causes the melt composition to be less than p. Appreciably larger differences are seen for "peak" melting temperatures calculated similarly from equilibrium n^*(peak). It happens that equilibrium $f_c = 0.14$ for all the model EB copolymers at T_m^p; this level of crystallinity noticeably decreases melt composition from p, contrary to the formulation of eq 5. We conclude that eq 5 is valid for the *final* melting of nonequilibrium crystals, because the melt has global composition p. Use of eq 5 at T_m^p, or at any other temperature in the melting range where crystallinity f_c, either equilibrium or nonequilibrium, is sensibly greater than zero, will return an apparent crystal thickness that is too small.

A different expression for the equilibrium T_m^c was proposed by Baur,[34] based on a statistical thermodynamic treatment of copolymer melting from Kilian:[31]

$$\frac{1}{T_m^c} = \frac{1}{T_m^0} - \frac{R}{\Delta H_u}(\ln p - 1/\bar{n}_t) \qquad \text{(A6)}$$

Again T_m^c is for melting infinitely thick crystals and a melt with global composition p. Here $\bar{n}_t = 1(2p(1-p))$ is the average sequence number of *all* segments, of both A and B types, in the copolymer. The additional term involving $\bar{n}_t$ reduces T_m^c considerably when compared with eq 2 in the text; for an ethylene copolymer with $p = 0.9$, the melting temperature calculated by eq A6 is 27 K below T_m^c from the Flory model.

While eq A6 has the apparently attractive feature that calculated equilibrium T_m^c corresponds better to experimental melting temperature than does the Flory model (eq 2), we believe that this is fortuitous and potentially misleading. It is widely recognized (see for instance refs 33 and 36) that the Kilian/Baur approach is based on each crystal being composed exclusively of n-sequences of one particular n. (In the Flory model for which the thermodynamic T_m^c is eq 2, a crystal of thickness n^*c is composed of sequences with $n \geq n^*$.) It is clear that such perfect partitioning of segments in the Kilian/Baur theory is even more difficult to achieve than equilibrium in the Flory sense. This unrealistic assumption nevertheless has the consequence of increasing the entropy of melting (due to additional entropy of mixing in the melt), which lowers the "equilibrium" melting temperature. The extra term $1/\bar{n}_t$ in eq A6 follows from applying Flory−Huggins lattice theory to the copolymer melt, where each n-sequence within a chain is treated as a discrete molecule of n repeat units. Because the entropy of an n-sequence covalently bonded in a long chain is *not* that of a chain of n monomers, the result of Baur[34] is incorrect.

Goldbeck-Wood[35] treats crystals formed from n-sequences of crystallizable A units in yet a different fashion. The starting point is the observation that Flory's result (eq 2 in text) is for equilibrium conditions that cannot be obtained in the laboratory. On the basis of an alternative approach to polymer crystallization kinetics, in which entropy dominates stem addition, Goldbeck-Wood evaluates the free energy and hence T_m^f of a lamellar crystal in equilibrium with the copolymer melt. The melting temperature can be written as

$$\frac{1}{T_m^f} = \frac{\dfrac{1}{T_m^0} - \dfrac{n_m - 1}{2}\dfrac{R}{\Delta H_u}(\ln p)}{1 - \dfrac{2\sigma_e a_o}{\Delta H_u n_m}} \qquad \text{(A7)}$$

This expression is distinguished from the Sanchez−Eby result (eqs 5 and 2) by the factor $(n_m - 1)/2$ in the numerator. The quantity n_m is an average sequence number of crystals stable at the melting temperature T_m^f, and hence is comparable to n^*(final) in Flory's treatment. However, the relevant sequence/crystal length n_m, which can be varied for a given copolymer, is determined from a (numerical) kinetic analysis. An unexpected result is the destablization of thick crystals (large n_m) because of an additional entropy penalty associated with finding a long n_m-sequence in the crystal. Inasmuch as melting does not reorder the monomer units within chains, this same entropy applies to a sequence in the melt and hence should not influence the thermodynamics of fusion. Equation A7 certainly predicts much lower "melting temperatures" than does the Sanchez−Eby model, but it does so with arguments that ignore the usual considerations of equilibrium between crystals and the melt.

In summary, the Sanchez−Eby[16] approach (eq 5 in text) is correct for *final* melting temperature T_m^f when comonomer is rejected from either equilibrium or nonequilibrium crystals. Baur's[34] result for the thermody-

namic melting point T_m^c (eq A6) suffers from unrealistic assumptions and an inappropriate description of mixing entropy. While this approach does predict T_m^c that is closer to experiment than the Flory result (eq 2), such a distinction does not imply that Baur's version of equilibrium is operative. We believe that experimental crystal thickness in random copolymers is dominated by kinetic factors. Analysis of melting temperatures in terms of Baur's and related treatments[36] may convey the misleading message that crystallization conforms to an unachievable "equilibrium". Goldbeck-Wood's[35] method does decouple (kinetic) crystallization from (thermodynamic) melting, but the final melting temperature T_m^f (eq A7) is too small.

References and Notes

(1) Wild, L. *Adv. Polym. Sci.* **1990**, *98*, 1.
(2) Mirabella, F. M.; Westphal, S. P.; Fernando, P. L.; Ford, E. A.; Williams, J. G.*J. Polym. Sci.: Part B: Polym. Phys.* **1988**, *26*, 1995.
(3) Krigas, T.; Carella, J.; Struglinski, M.; Crist, B.; Graessley, W. W.; Schilling, F. C. *J. Polym. Sci.: Polym. Phys. Ed.* **1985**, *23*, 509.
(4) Hosoda, S. *Polym. J.* **1988**, *20*, 383.
(5) Alamo, R. G.; Mandelkern, L. *Thermochim. Acta* **1994**, *238*, 155.
(6) Fu, Q.; Chiu, F.-C.; McCreight, K. W.; Guo, M.; Tseng, W. W.; Cheng, S. Z. D.; Keating, M. Y.; Hsieh, E.; DesLauriers, P. J. *J. Macromol. Sci.—Phys.* **1997**, *B36*, 41.
(7) Flory, P. J. *Trans. Faraday Soc.* **1955**, *51*, 848.
(8) Mandelkern, L.; Alamo, R. G. In *Physical Properties of Polymers Handbook*; Mark, J. E. Ed.; American Institute of Physics: Woodbury, NY, 1996, Chapter 11.
(9) Hoffman, J. D.; Miller, R. L. *Polymer* **1997**, *38*, 3151.
(10) Clark, E. S. In *Physical Properties of Polymers Handbook*; Mark, J. E., Ed.; American Institute of Physics: Woodbury, NY, 1996; Chapter 30.
(11) Darras, O.; Séguéla, R. *Polymer* **1993**, *34*, 2946.
(12) Lu, L.; Alamo, R.; Mandelkern, L. *Macromolecules* **1994**, *27*, 6571.
(13) Kilian, H. G. *Thermochim. Acta* **1994**, *238*, 113 and references therein.
(14) Pakula, T. *Polymer* **1982**, *23*, 1300.
(15) Wang, P.; Woodward, A. *Macromolecules* **1987**, *20*, 1818.
(16) Sanchez, I. C.; Eby, R. K. *Macromolecules* **1975**, *8*, 639.
(17) Rachapudy, H.;. Smith, G.; Raju, V.; Graessley, W. W. *J. Polym. Sci.: Polym. Phys. Ed.* **1979**, *17*, 1211.
(18) Howard, P. R.; Crist, B. *J Polym. Sci.: Part B: Polym. Phys.* **1989**, *27*, 2269.
(19) Pérez, E.; VanderHart, D. L.; Crist, B.; Howard, P. R. *Macromolecules* **1987**, *20*, 78.
(20) Crist, B.; Williams, D. N. *J. Macromol. Sci.—Phys.*, in press
(21) Richardson, M. J.; Flory, P. J.; Jackson, J. B. *Polymer* **1963**, *4*, 221.
(22) Alamo, R. G.; Mandelkern, L. *Macromolecules* **1991**, *24*, 6480.
(23) Ergoz, E.; Fatou, J. G.; Mandelkern, L. *Macromolecules* **1972**, *5*, 147.
(24) Wissler, G. Ph.D. Thesis, Northwestern University, 1982.
(25) Alamo, R.; Domszy, R.; Mandelkern, L. *J. Phys. Chem.* **1984**, *88*, 6587.
(26) Voight-Martin, I. G.; Alamo, R.;. Mandelkern, L. *J. Polym. Sci., Part B: Polym. Phys.* **1986**, *24*, 1283.
(27) Crist, B.;. Wignall, G. D. *J. Appl. Crystallogr.* **1988**, *21*, 701.
(28) Crist, B.; Nicholson, J. C. *Polymer* **1994**, *35*, 1846.
(29) Wunderlich, B. *J. Chem. Phys.* **1958**, *29*, 1395.
(30) Keller, A.; Goldbeck-Wood, G. In *Comprehensive Polymer Science*, Second Supplement; Allen, G., Aggarwal, S. L., Russo, S., Eds., Elsevier Science: Tarrytown, NY, 1996; Chapter 7.
(31) Kilian, H. G. *Kolloid Z. Z. Polym.* **1965**, *202*, 97.
(32) Baur, H. *Kolloid Z. Z. Polym.* **1965**, *203*, 97.
(33) Wunderlich, B. *Macromolecular Physics*; Academic Press: New York, 1976; Vol. 2; pp 259−271.
(34) Baur, H. *Makromol. Chem.* **1966**, *98*, 297.
(35) Goldbeck-Wood, G. *Polymer* **1992**, *33*, 778.
(36) Wendling, J.; Suter, U. W. *Macromolecules* **1998**, *31*, 2516.

MA9816362